9112 *Biochemistry* **2009,** *48,* 9112–9121
DOI: 10.1021/bi9008566

BIOCHEMISTRY
including biophysical chemistry & molecular biology
Article

Conserved Leucine Residue in the Head Region of Morbillivirus Fusion Protein Regulates the Large Conformational Change during Fusion Activity

Philippe Plattet,*[,‡,#] Johannes P. M. Langedijk,[∥,#] Ljerka Zipperle,[‡] Marc Vandevelde,[§] Claes Örvell,[⊥] and Andreas Zurbriggen[‡]

[‡]*Department of Clinical Research and Veterinary Public Health and* [§]*Division of Neurology, Vetsuisse Faculty, University of Bern, Bern, Switzerland,* [∥]*Pepscan Therapeutics BV, 8203 AB, P.O. Box 2098, Lelystad, The Netherlands, and* [⊥]*Laboratory of Clinical Virology, Karolinska University Hospital Huddinge, Stockholm, Sweden.* [#]*These authors contributed equally to this study.*

Received May 20, 2009; Revised Manuscript Received August 25, 2009

ABSTRACT: Paramyxovirus cell entry is controlled by the concerted action of two viral envelope glycoproteins, the fusion (F) and the receptor-binding (H) proteins, which together with a cell surface receptor mediate plasma membrane fusion activity. The paramyxovirus F protein belongs to class I viral fusion proteins which typically contain two heptad repeat regions (HR). Particular to paramyxovirus F proteins is a long intervening sequence (IS) located between both HR domains. To investigate the role of the IS domain in regulating fusogenicity, we mutated in the canine distemper virus (CDV) F protein IS domain a highly conserved leucine residue (L372) previously reported to cause a hyperfusogenic phenotype. Beside one F mutant, which elicited significant defects in processing, transport competence, and fusogenicity, all remaining mutants were characterized by enhanced fusion activity despite normal or slightly impaired processing and cell surface targeting. Using anti-CDV-F monoclonal antibodies, modified conformational F states were detected in F mutants compared to the parental protein. Despite these structural differences, coimmunoprecipitation assays did not reveal any drastic modulation in F/H avidity of interaction. However, we found that F mutants had significantly enhanced fusogenicity at low temperature only, suggesting that they folded into conformations requiring less energy to activate fusion. Together, these data provide strong biochemical and functional evidence that the conserved leucine 372 at the base of the HRA coiled-coil of F^{wt} controls the stabilization of the prefusogenic state, restraining the conformational switch and thereby preventing extensive cell−cell fusion activity.

Paramyxoviruses are enveloped nonsegmented negative strand RNA viruses. Injection of the genetic information into target cells is achieved by a fusion process between virus and cell, which is sustained by the concerted action of two viral membrane-bound glycoproteins. The attachment protein (H,[1] HN, or G, depending on the viral genus) is thought to bind a host cell surface receptor in turn activating the fusion (F) protein, which will then undergo drastic structural rearrangements ultimately leading to plasma membrane fusion activity (*1*, *2*). In addition, both viral surface glycoproteins are involved in mediating fusion between two adjacent cells. Viral-induced cell−cell fusion eventually leads to multinucleated cell formation (also termed syncytium formation) and finally to cell lysis.

Persistent infection with canine distemper virus (CDV), a paramyxovirus closely related to measles virus (MV), produces a multiple sclerosis-like disease in carnivores (*3*). The induction of a persistent infection in the central nervous system (CNS) is tightly linked to the very limited capacity of the virulent CDV to induce cell−cell fusion, in sharp contrast to attenuated CDV strains, which induce ample syncytium formation (*4*, *5*). Our earlier studies in cell cultures demonstrated that extremely limited syncytium formation mediated by A75/17-CDV, a virulent viral strain which is directly derived from canine tissues, is partly controlled by the fusion protein (*4*, *6*−*8*). Understanding the molecular mechanisms that control limited fusion activity in the wild-type CDV strain is therefore essential for unraveling the pathogenesis of the disease.

The F protein is first synthesized as a single precursor protein (F_0) in the endoplasmic reticulum compartment, folds as a homotrimer, and is glycosylated. Next, F trimers heterooligomerize with the receptor-binding protein H and, once in the Golgi apparatus, are further cleaved into two disulfide-linked F_1 and F_2 subunits prior to reaching the plasma membrane (*9*). F_1 contains two hydrophobic regions, the N-terminal fusion peptide and the transmembrane domain, as well as two heptad repeat regions (HRA and HRB). The processed and surface-bound F/H complex represents the actual potentially fusion-active complex of most *Paramyxoviridae*.

The native F protein initially folds into a high energy-containing metastable state, which upon triggering refolds into an irreversible postfusion form associated with a lower energy. According to recent X-ray studies on paramyxovirus parainfluenza virus 5 (PIV5), the metastable form exhibits a globular head containing three domains (DI−DIII) attached to a stalk domain consisting of a triple-stranded coiled coil formed by the

*To whom correspondence should be addressed. Phone: +4131 631 26 48. Fax: ++4131 631 25 38. E-mail: philippe.plattet@itn.unibe.ch.

[1]Abbreviations: CDV, canine distemper virus; OP, Onderstepoort CDV vaccine strain; MV, measles virus; PIV5, parainfluenza virus 5; HIV, human immunodeficiency virus; F, fusion protein; FGps, fusion glycoproteins; H, hemagglutinin protein; IS, intervening sequence; HR, heptad repeat region; HB, helical bundle domain; DIII, domain III; env/GP160, human immunodeficiency virus fusion glycoprotein; HA, influenza virus fusion glycoprotein; 6HB, six-helix bundle; CBF1, conserved block region in the membrane-anchored F subunit; GFP, green fluorescent protein; RFP, red fluorescent protein; MAbs, monoclonal antibodies; SLAM, signaling lymphocyte activation molecule; Tryp, trypsin; MOI, multiplicity of infection.

 Published on Web 08/25/2009

HRB (*10*). Conversely, HRA is located at the top of the globular head domain and is composed of 11 distinct segments which are trapped in a crumpled, spring-loaded conformation. Upon activation, extensive refolding of HRA leads to the formation of an extended triple-stranded coiled-coil structure and insertion of the hydrophobic fusion peptide into the target plasma membrane. Then, HRB is believed to swing around the globular head domain and to bind into the grooves of the HRA coiled coil, which consequently generates the highly stable six-helix bundle (6HB). The latter structure is thought to be directly coupled to membrane merging (*11*). Both paramyxovirus HR domains in F have been intensively studied, highlighting key amino acids regulating the fusion process (*12*, *13*). In addition, peptides spanning both HR domains were shown to be potent inhibitors of viral replication, most likely by inactivating F refolding through binding to their complementary sequence at distinct stages of the fusion cascade (*14*−*20*).

Besides both heptad repeat regions, the paramyxovirus F protein shares structural similarities such as the fusion peptide, the transmembrane, and the cytoplasmic tail domains (all known to control the fusion process (*12*, *21*−*25*)), with other class I viral fusion glycoproteins (FGps) such as HIV env/GP160 and influenza virus hemagglutinin (HA). Particular to paramyxovirus fusion glycoproteins (FGp), however, is an extremely long intervening sequence (IS; more than 250 amino acids) located between both HR domains of the membrane-anchored F_1 subunit. Apart from a recent report on a conserved block region (CBF_1) located in IS of Hendra virus and PIV5 FGps, which documented a role of this domain in modulating fusion activity (*26*), not much is known about the function of this long intervening sequence in the regulation of the fusion process.

We recently reported that one substitution (L372W) in IS resulting from multiple passages rendered wild-type CDV hyperfusogenic (*8*). In the present study we conducted a detailed mutational analysis of position 372 in the CDV F-A75/17 protein (referred to as F^{wt}) to investigate the molecular mechanisms by which the highly conserved leucine residue was controlling limited fusion activity. Using viral protein expression studies, quantitative fusion assays, conformation-dependent antibody binding studies, and temperature dependence of fusion activation, our data demonstrate that the conserved leucine residue located in the long intervening sequence in between HRA and HRB in F^{wt} plays a critical role in controlling the fusion process. We found that L372 was part of a network of residues involved in regulating the folding of F^{wt} into a specific prefusion conformational state, which is characterized by an elevated activation energy threshold, thereby limiting plasma membrane fusion activity.

MATERIALS AND METHODS

Cell Cultures and Viruses. Vero and Vero cells expressing SLAM and the green fluorescent protein (Vero-SLAM-GFP) were grown in Dulbecco's modified Eagle's medium (Gibco, Invitrogen) with 10% fetal calf serum at 37 °C in the presence of 5% CO_2. Bsr-T7/5 cells were grown as the Vero cells, except that the medium was supplemented with 2% FCS and 0.5 mg/mL G-418. The MVA-T7 recombinant vaccinia virus was used for a quantitative cell−cell fusion assay and was obtained from B. Moss, NIH, Bethesda, MD.

Construction of Expression Plasmids. The plasmids pCI-$F^{A75/17}$, pCI-H^{OP}, and pCI-H^{wt} cloned in the mammalian expression vector pCI (Promega) were described previously (*27*). Plasmid $hscF^{wt}$ bearing an heterogeneous signal peptide was previously described (*8*). We fused the influenza hemagglutinin tag sequence (HA) to the cytoplasmic tail of $hscF^{wt}$, generating $hscF^{wt}$-HA (referred to in this study as F^{wt}). The red fluorescent protein gene (kindly gift by Dominique Garcin, University of Geneva) was cloned into the pCI plasmid. All plasmids sequences were confirmed by automated nucleotide sequence analysis.

The lentivirus vector pRRL has been described elsewhere (*28*) and was kindly provided by Patrick Salomon, University of Geneva). Stock of lentivirus vectors was generated in 293T/17 cells as previously described (*28*).

Transfections and Luciferase Reporter Gene Content Mix Assay. Vero cells, in six-well plates at 90% confluency, were cotransfected with 2 μg of the CDV F constructs and 1 μg of pCI-H^{OP} or pCI-H^{wt} using 9 μL of Fugene HD (Roche) according to the manufacturer's protocol. Pictures were taken 24 h posttransfection with a confocal microscope (Olympus).

The quantitative fusion assay was performed as described previously (*8*, *29*). Briefly, Vero cells cotransfected with the F and H expression plasmids and 0.1 μg of pTM-Luc (kindly provided by Laurent Roux, University of Geneva). In parallel, separate six-well plates of Vero cells at 30% confluency were infected with MVA-T7 (*30*) at a multiplicity of infection (MOI) of 1. After O/N incubation, both cell populations were mixed. Four hours later, the cells were lysed using Bright Glo lysis buffer (Promega), and the luciferase activity was determined using a luminescence counter (PerkinElmer Life Sciences) and the Britelite reporter gene assay system (PerkinElmer Life Sciences).

Western Blotting. Western blots were performed as previously described (*8*). Transfected cells were washed twice with cold PBS before adding 150 μL of lysis buffer [10 mM Tris, pH 7.4, 150 mM NaCl, 1% deoxycholate, 1% Triton X-100, 0.1% sodium dodecyl sulfate (SDS)] with complete protease inhibitor (Roche Biochemicals). After incubation for 20 min at 4 °C, the lysates were cleared by centrifugation at 5000*g* for 15 min at 4 °C, and the supernatant was mixed with an equal amount of 2× Laemmli sample buffer (Bio-Rad) containing 100 mM dithiothreitol, subsequently boiled at 95 °C for 5 min, and fractionated on 8% or 10% SDS−polyacrylamide gels under denaturing conditions. Separated proteins were transferred to nitrocellulose membranes by electroblotting. The membranes were then incubated with the polyclonal rabbit anti-CDV F or H antisera (*27*). Following incubation with a peroxydase-conjugated secondary antibody, the membranes were subjected to an enhanced chemiluminescence (ECL) kit (Amersham Pharmacia Biotech) according to the manufacturer's instructions.

Surface Biotinylation. Surface biotinylation was performed as previously described (*8*). Briefly, 24 h posttransfection, cells were washed in cold PBS and incubated in PBS with 0.5 mg/mL sulfo-succinimidyl-2-(biotinamido)ethyl-1,3-dithiopropionate (Pierce) for 20 min at 4 °C, washed three times with 0.5 M glycine in PBS, and further incubated in 1 mL of 0.5 M glycine−PBS for 20 min at 4 °C. Samples were scraped into 150 μL of lysis buffer [10 mM Tris, pH 7.4, 150 mM NaCl, 1% deoxycholate, 1% Triton X-100, 0.1% sodium dodecyl sulfate (SDS)] containing protease inhibitors (Roche; complete mix), and the lysates were cleared by centrifugation for 20 min at 20000*g* and 4 °C. The biotinylated proteins were adsorbed to Sepharose-coupled streptavidin (Amersham Pharmacia Biotech) O/N at 4 °C and washed three times in lysis buffer, before 30 μL of 2× Laemmli sample buffer (Bio-Rad) containing 100 mM dithiothreitol was added. The samples then underwent Western blot analysis as described above.

Coimmunoprecipitation. At 24 h posttransfection, the cells were washed three times with cold PBS and lysed in coimmunoprecipitation buffer [50 mM HEPES (pH 7.2), 10 mM dodecyl β-D-maltoside (Sigma), 150 mM NaCl] containing protease inhibitors (Roche Applied Science) for 45 min on ice. Cleared lysates (20000*g*, 20 min, 4 °C) were incubated for 3 h with a mixture of three anti-CDV-H monoclonal antibodies (3900, 1347, (*31*) and 1C42H11, VMRD) followed by O/N incubation with immunoglobulin G-coupled Sepharose beads. The precipitates were washed three times each in coimmunoprecipitation buffer, followed by adding 2× Laemmli sample buffer (Bio-Rad) containing 100 mM dithiothreitol. The samples were then subjected to Western blot analysis as described above using either the polyclonal anti-H or the anti-F antibody (*27*).

Generation of Vero-SLAM Cells Constitutively Expressing the GFP Protein. Vero-SLAM cells (kind gift from V. von Messling, University of Quebec) were transduced with pRRL lenti vectors at an MOI of 5. Consequently, a highly GFP-expressing clone was selected by limiting dilution and was used for further experiments.

GFP Transfer Fusion Assay for Temperature Dependence of F Activation. To measure the temperature dependence of fusion induction by the different CDV F protein mutants, we used Vero-SLAM-GFP cells. Effector BsrT7 cells (BsrT7 cells showed extremely low induction of syncytia with all F proteins after O/N incubation) were transfected with the various F constructs and H^{wt} together with pCI-RFP. After 24 h of incubation, Vero-SLAM-GFP cells were overlaid for 15 min on effector cells at 4 °C to allow efficient binding. Fusion was promoted by incubation for 20 min at 25, 32, 37, or 43 °C followed by repeated washing with cold PBS and incubation on ice. GFP transfer was visualized using a confocal laser scanning fluorescence microscope (Olympus). Random fields were captured using the IPLab 3.7 software (Olympus). By merging red and green images, yellow cells were counted in defined area of at least five different fields of view.

Flow Cytometry. To determine the conformation of F proteins, Vero cells were first transfected with 1 μg of F-expression plasmids. One day posttransfection, unfixed cells were washed twice with ice-cold PBS and subsequently stained with one of the various anti-CDV-F MAbs (1:1000) for 1 h at 4 °C. The anti-CDV-F MAbs 3633, 4068, and 4985 were previously described (*31*). This was followed by intensive washes with ice-cold PBS and incubation of the cells with Alexa-fluor 488-conjugated secondary antibody (1:300) for 1 h at 4 °C. Cells were washed five times with ice-cold PBS and consequently detached from the wells by adding PBS-EDTA (50 mM) for 30 min at 37 °C. The mean fluorescence intensity of 10000 cells was then measured by using a FACSCalibur flow cytometer.

Homology Modeling. Homology modeling was performed using the sequence alignment of hPIV5-F and CDV-$F^{A75/17}$ and the homologous template of the native F structure of hPIV5 (*10*) using the automated protein-modeling software on the SWISS-MODEL protein-modeling server (*32*, *33*). According to the alignment, only very few insertions and deletions were necessary to construct the model. Model verification was done using WhatCheck (*34*). Accuracy of the model was very high because of the high sequence similarity of CDV-F with the template (59%). Modeling was performed three times using the three separate monomers of hPIV5-F with very similar results. The three resulting CDV-F monomers were merged into a trimer which is the most likely quaternary structure of the CDV-F.

RESULTS

The Highly Conserved Leucine 372 Residue Is Located in the Core Head Structure of the Metastable F. We recently demonstrated that a tryptophan (W) substitution at position L372 in the long intervening sequence (IS) of the CDV F protein caused a striking enhancement in wild-type virus-mediated fusogenicity (*8*).

To locate the position of the conserved leucine residue 372 in the IS domain of the metastable F, we generated a homology structural model based on the crystal structure of the related paramyxovirus hPIV5 F protein (*10*). Based on this model, it appeared that residue L372 is located in the helical bundle (HB) region of the domain III core in the F globular head. In the metastable F structure, HB is composed of four α-helices and four turns and is located C-terminal to the heptad repeat region A (HRA, Figure 1A). No defined function has been so far attributed to the HB domain of any paramyxovirus F protein. Interestingly, part of the HB region makes contacts with the H4 α-helix of the HRA. H4 is one of the 11 distinct HRA segments that are found in the spring-loaded metastable F conformation (Figure 1B). In fact, H4 is the basal helix on top of which all other segments will unroll upon F activation to generate the triple-stranded coiled-coil structure. Furthermore, the model predicts that L372 in HB of one monomer binds L326 in H4 of another monomer (Figure 1C), thus suggesting that residue L372 potentially is involved in F protein folding and/or stabilization.

Expression, Processing, and Cell Surface Targeting of F L372 Mutants. To determine whether L372 is indeed involved in F^{wt} protein folding and/or stability, we introduced aromatic (W and F), aliphatic (G, V, A), or a polar (N) residue at position 372 in CDV F^{wt}. In the present report, we used a wild-type F protein-expressing plasmid bearing the signal peptide of the human secretory component in order to exclusively dissect the role of the mutations in correlation to F_1/F_2-mediated cell−cell fusion activity. In addition, we fused an HA-tag sequence to the cytoplasmic tail of the F protein to allow efficient pull-down experiments (referred in this study as F^{wt}, Figure 1A). The tag did not show any modulation in F functionality (data not shown).

Expression, processing, and cell surface targeting of all F mutants were then evaluated after cotransfection of the various F proteins and wild-type H-expressing plasmids in Vero cells. Immunoblotting using a polyclonal anti-F antibody followed by densitometric analyses revealed that all F proteins were expressed and processed (Table 1). While the F L372G mutant showed about 50% reduction in total protein expression, other mutants were not characterized by drastic differences relative to F^{wt} (Table 1). Cleavage efficiencies of the different F_0 precursor proteins were then measured as a ratio of $F_1/(F_0 + F_1)$. Here again the L372G and to some extent the L372N F mutants showed moderate deficiencies in F_0 processing as compared to F^{wt}, whereas the others precursors were properly cleaved (Table 1).

Surface biotinylation assay was next performed to discriminate between plasma membrane-bound and intracellular F products. Densitometric analyses of immunoblots documented that all F mutants reached the cell surface, though the various F_1 bands revealed that expression levels of some mutants differed from the one of F^{wt}. While the L372G and L372F mutants exhibited a substantial reduction in cell surface expression (43% and 60%, respectively), the remaining mutants were only slightly less expressed at the cell surface as compared to F^{wt} (Table 1). Taken

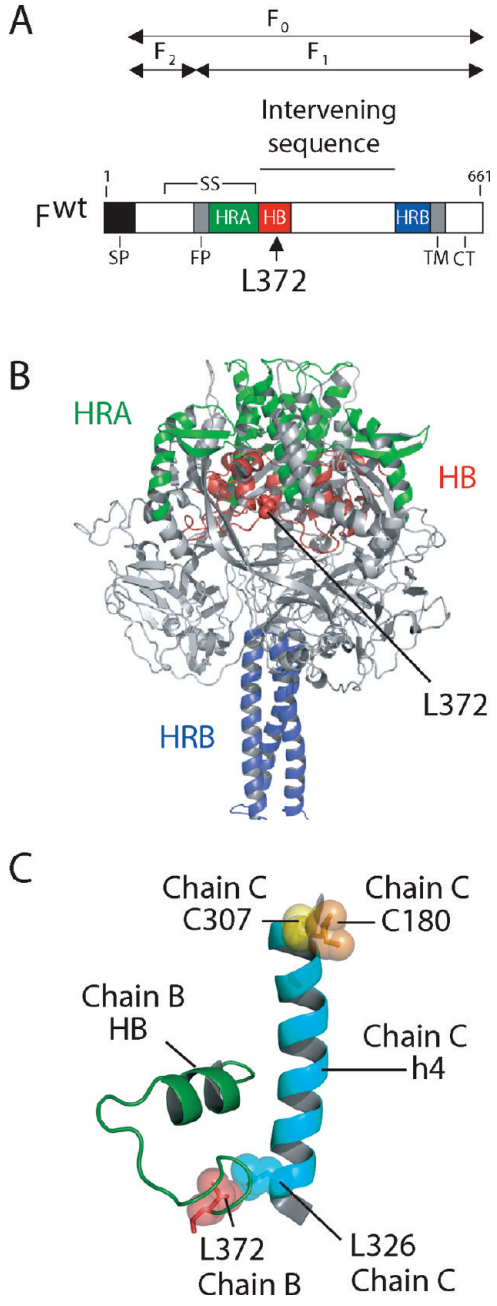

FIGURE 1: Localization of residue L372 in wild-type CDV F. (A) The main domains of CDV F are shown: signal peptide of the human secretory component (hscSP), the fusion peptide (FP), both heptad repeats (HRA in blue and HRB in green), the helical bundle (HB in red), the transmembrane domain (TM), and the cytoplasmic tail (CT). The position of the leucine residue 372 in the intervening sequence (IS) is shown. The disulfide bond formed between the F_1 and F_2 subunits is also represented. (B) CDV F^{wt} structural model showing the location of L372 at the interface of the monomeric chains. The HRA (green), HRB (blue), and HB (red) are represented. (C) Close-up view of the interaction between residue L372 (red) in the HB (chain B) and residue L326 (cyan) in the H4 helix (chain C). Residues C180 and C307 in H4 are also represented. Figures were generated using PyMOL v0.99 and color coded for clarification.

together, these data suggest that, except for the F L327G mutant, F protein expression, processing, and transport competence were not fundamentally affected by mutating L372.

Mutating the Conserved Leucine Residue of CDV F^{wt} into Alanine, Tryptophan, or Asparagine Confers Fusion Activity in Vero Cells. Cell−cell fusion in paramyxovirus is mediated by viral F and H glycoproteins as well as a specific

Table 1: Expression of Wild-Type and Mutant CDV F Proteins[a]

CDV wt F and mutants	expression: total[b]	expression: surface[c]	cleavage efficiency[d]
L372 (wt)	100	100	100
L372W	87 ± 9	78 ± 10	78 ± 14
L372A	117 ± 24	88 ± 24	81 ± 18
L372V	77 ± 12	70 ± 23	79 ± 7
L372G	51 ± 34	43 ± 9	57 ± 15
L372F	70 ± 15	60 ± 23	71 ± 5
L372N	73 ± 23	59 ± 19	65 ± 18

[a]CDV F proteins expressed from pCI DNA in Vero cells for 24 h. [b]Total expression as determined by the total amount of F: (F_0 + F_1). Data are normalized to CDV wild-type F (%). [c]Cell surface expression as determined by biotinylation assay. Data are normalized to CDV wild-type F (%). [d]Cleavage efficiency as measured by determining the ratio $F_1/(F_0 + F_1)$. Data are normalized to CDV wild-type F (%). Densitometric analyses were performed with the AIDA software package.

receptor on target cells. Modification of either one of these three central players will inevitably modify the efficiency of the fusion process. In order to create optimal conditions to objectively assess the effect of F mutants on fusion efficiency, Vero cells expressing the canine CD150/SLAM receptor might be employed, since previous studies have demonstrated that the SLAM/H^{wt}/F^{wt} tripartite combination was sufficient to promote syncytia formation in several cell lines (*7*, *35*). Alternatively, the receptor-binding protein of the attenuated Onderstepoort CDV strain (H^{OP}) might also be used to induce syncytium formation in cells lacking SLAM expression, most probably by binding with high avidity to a yet unidentified cell surface receptor (*7*, *36*).

Thus, in order to investigate whether F L372 mutants when combined to H^{wt} could induce cell−cell fusion in the absence of SLAM, F^{wt} (or derivatives) expressing plasmids were cotransfected with wt H in Vero cells. Fusogenicity induced by the various F proteins was determined by a luciferase reporter gene content mix assay, and values were normalized to F^{wt} expression. Consistent with previous results (*8*), the combination of the parental nonmutated F protein with H^{wt} did not induce fusion in Vero cells, and indeed values barely exceeded background levels (Figure 2A). Similar results were obtained with L372 V, L372F, and L372G F mutants. Conversely, induction of fusion was achieved with the aromatic L372W, the aliphatic L372A, and the polar L372N F mutants, thus demonstrating for the first time that single point mutants in F^{wt} in combination with H^{wt} mediate fusion in the absence of the SLAM receptor (Figure 2A). In addition, these results indicate that H^{wt} does bind, perhaps with low affinity, to a yet unidentified CDV receptor in Vero cells, since transfection of all F proteins alone did not exhibit any fusion activity (data not shown). Microscopic assessment of syncytium formation in Vero cells confirmed the results obtained in the content mix assay, although syncytia detected in the transfected cells with F mutants L372W, L372A, and L372N were very rare and small at the most containing 10−15 nuclei (Figure 2B).

In a subsequent series of experiments, fusion assays were repeated using the attachment protein of the attenuated OP-CDV strain (H^{OP}). Importantly, using this receptor-binding protein, syncytia formation was indeed elicited in all F/H combinations, though to various extents (not shown). Nevertheless, since in this environment all F mutants were fusogenic,

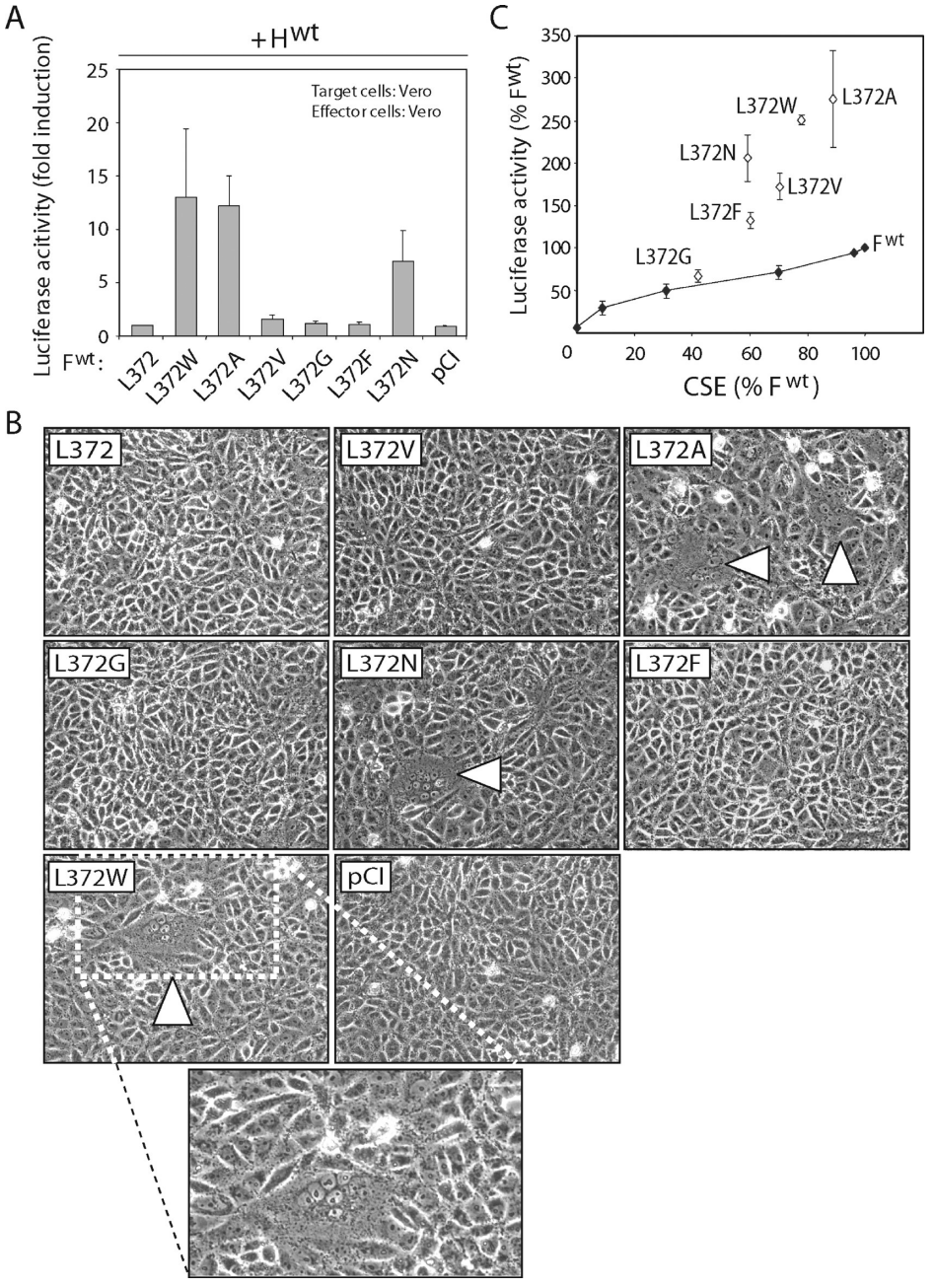

FIGURE 2: Fusogenicity induced by the various F proteins. (A) Luciferase gene content mix assay. For quantitative fusion assay, Vero cells were either infected with MVA-T7 (MOI of 1) or transfected with the different F proteins, a plasmid encoding H^{wt} and a plasmid containing the luciferase reporter gene under the control of the T7 promoter. Twelve hours after transfection, both cell populations were mixed and seeded into fresh plates. After 5 h at 37 °C, fusion was quantified by measuring the luciferase activity produced. For each experiment, the value for the F^{wt}/H^{wt} combination was set to 100%. Means and standard deviations of three independent experiments in duplicate are shown. (B) Syncytium formation after cotransfection of the cells with plasmid DNA encoding CDV H^{wt} and F^{wt} or derivative F mutant proteins. Mock transfected cells (pCI) received CDV H^{wt} encoding plasmid and empty vector; representative fields of view were photographed 24 h posttransfection. (C) F mutants induced hyperfusogenic phenotype at F^{wt}-like surface expression. The solid line represents the values of cell surface expression (CSE) versus fusion of increasing amounts of transfected F^{wt} DNA. CSE of F^{wt} expressed with H^{OP} was determined by surface biotinylation. Biotinylated F proteins from transfected Vero cells were precipitated overnight with streptavidin coupled to agarose beads, separated by reducing SDS−PAGE, and blotted onto nitrocellulose membranes. The identical polyclonal anti-F antibody was employed to reveal the F antigenic materials. Then, for each F cell surface expression condition, fusogenicity was measured using the luciferase gene content mix assay, as desrcibed in panel A. Means and standard deviations of three independent experiments in duplicate are shown. The value of 2 μg of transfected DNA was normalized to 100% fusion and 100% surface expression. Then, fusogenicity F mutants (open squares) coexpressed with H^{OP} were determined as described in panel A. Values of F mutants' CSE were determined by cell surface biotinylation assay. Values were finally plotted on the graph.

we sought to correlate F-mediated cell−cell fusion activity with cell surface expression. To accurately address this question, cell surface expression was controlled by transfecting decreasing amounts of wild-type F-expressing plasmids in Vero cells. While fusogenicity was assessed by luciferase content mix assay, cell surface expression was investigated by surface biotinylation, and both values were plotted on a graph (Figure 2C, filled black line). Next, values obtained for all F mutants were added. Figure 2C clearly indicates that, except F L372G, all other F mutants caused enhanced fusion activity when expressed at similar cell surface densities from that of wild-type F. Furthermore, the three F mutants (W, A, and N) that could achieve syncytia formation in

the presence of H^{wt} were also the most hyperfusogenic when combined to H^{OP}. Altogether, these results indicated that although substituting the leucine residue in the core structure of the F^{wt} protein did not mediate increased cell surface expression, fusogenicity was nevertheless substantially enhanced, and this, regardless of the origin of the receptor-binding protein employed.

F L372 Mutants Exhibited Modulated Reactivity for Three Different Conformational Epitope-Recognizing Monoclonal Antibodies. To assess any potential conformational changes in F proteins, we took advantage of previously generated anti-CDV-F monoclonal antibodies (*31*). Three monoclonal antibodies (MAbs) were employed (3633, 4068, and 4985), since they did not react with the unfolded F^{wt} protein in immunoblots, whereas they did bind the F^{wt} protein in immunoprecipitation (IP) assays (ref *31* and personal observations). Moreover, it had been initially demonstrated that these three MAbs recognized different, nonoverlapping epitopes (*31*), indicating that these antibodies presumably recognize three distinct conformation-dependent epitopes on the F structure.

To investigate whether conformational modifications in F mutants were present at the cell surface, flow cytometry was employed of F- and H-expressing cells. Mean fluorescence intensities were then normalized to the total amount of mutants F expressed at the cell surface (obtained in the cell surface biotinylation assay). Results illustrated in Figure 3A indicate that all F mutants exhibited enhanced MAbs binding avidity. Interestingly, hyperfusogenic F mutants revealed by luciferase reporter gene content mix and syncytium formation assays correlated with higher MAb binding avidity (see F mutants L372W, L372A, and L372N; Figure 3A). In contrast, in an unanticipated manner, the hypofusogenic F L372G mutants caused the most spectacular increase in MAb binding efficiency.

Next, we expressed the various F proteins alone to investigate whether conformational changes were strictly dependent on the presence of the receptor-binding H protein. Values were normalized to the total amount of surface-bound F proteins expressed in the absence of H (as determined by surface biotinylation assay; Figure 3B, bottom panel). Figure 3B documents that the most hyperfusogenic F mutants retained enhanced binding to all three CDV-F MAbs in the absence of the H protein. However, except for F L372G, values obtained for MAb binding reactivity for all other mutants were less increased than the one recorded in the presence of H, suggesting that the receptor-binding protein can promote MAb binding reactivity of the various F mutants. While F mutants L372 V and L372F elicited only a very slight increase in MAb binding avidity, F mutants L372W, L372A, L372N, and L372G presented a substantial increase. Intriguingly, the least fusogenic F mutant (L372G) remained the most hyperreactive F protein with all three CDV-F MAbs.

Taken together, flow cytometry analysis of surface-expressed F proteins strongly supports the notion that modifying the highly conserved leucine residue in the core of the globular head structure results in conformational changes.

Interaction of F Mutants with the Receptor-Binding Protein H. According to current understanding of the paramyxovirus fusion mechanism, upon binding to the host cell surface receptor, H undergoes conformational changes, which subsequently trigger the metastable F protein to unfold. Thus, F/H interaction is probably of crucial importance in modulating fusion activity (*37*−*39*). To determine whether the overall structural integrities of the modified F L372 mutants' metastable

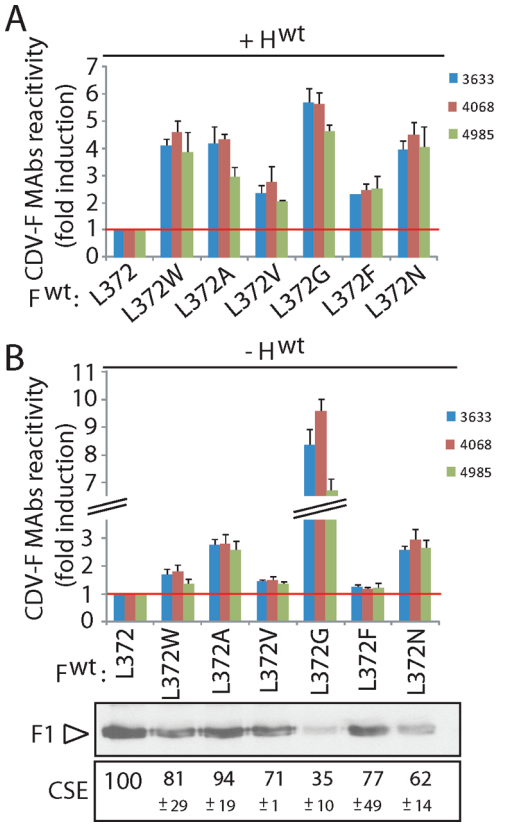

FIGURE 3: F L372 mutants exhibit conformational modification. (A) Monoclonal 3633, 4068, and 4985 anti-CDV-F antibodies binding to F proteins expressed in Vero cells in the presence of H^{wt}, as detected by flow cytometry. (B) Monoclonal 3633, 4068, and 4985 anti-CDV-F antibodies binding to F proteins expressed in Vero cells in the absence of H^{wt}, as detected by flow cytometry. Values of mean fluorescence intensities of all F proteins were normalized to the total amount of the various F proteins' density at the cell surface (obtained in surface biotinylation assay). Means and standard deviations of three independent experiments in duplicate are shown. Densitometric analysis was performed using the AIDA software package.

states were substantially modified, strength of F/H interaction was investigated. To this aim, co-IP assays from F^{wt} (or derivatives) and H^{wt} cotransfected in Vero cells were performed from total cell extracts.

Assessment of F/H interaction was undertaken using a mixture of anti-H MAbs (3900 and 1347 (*31*) as well as a commercially available anti-CDV-H 1C42H11) to immunoprecipitate the F/H complexes, which was subsequently followed by detection of F antigenic materials with a rabbit anti-F polyclonal antibody in Western blot analysis. While anti-H MAbs 3900 and 1C42H11 efficiently pulled down H^{wt} in IP assays but did not reveal any H protein bands in immunoblot analyses, the anti-H mAb 1347 did exhibit positive signals both in IP and in immunoblot assays (not shown). Results in Figure 4 illustrated that when wild-type F/H complexes were pulled down with the anti-H MAbs, the unprocessed F_0 precursor was readily detected, whereas only a few processed F_1 could be observed (Figure 4, lane 3), in agreement with recent results (*25*, *38*). In addition, critical controls are shown. The first pair of lanes demonstrated that F^{wt} did not co-IP when F^{wt} or H^{wt} was omitted from the transfection mixtures, thus validating the co-IP assay (Figure 4, lanes 1 and 2). Importantly, F/H avidity of interaction was not drastically reduced in the case of the hyperfusogenic F mutants (Figure 4, lanes 4, 5, and 9). These results are not unexpected,

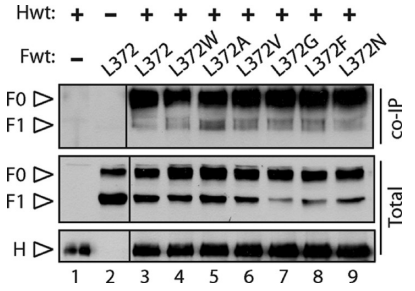

FIGURE 4: Coimmunoprecipitation assays (Co-IP) show that all F mutants efficiently interact with H. Lysates of cotransfected Vero cells with the various F-expressing or empty plasmids (pCI) together with H^{wt}-expressing or empty plasmids (pCI) were first immunoprecipitated (IP) with a mixture of three anti-CDV-H MAbs (3900, 1347, and 1C42H11), followed by protein G−Sepharose treatment. Proteins were then subjected to Western blot using a polyclonal anti-F antibody to detect the F antigenic materials. Co-IP F (upper panel) was detected in comparison with F present in the lysates prior to IP by Western blot using a polyclonal anti-F antibody (middle panel). To detect total H proteins, Western blots were performed with lysates taken prior to IP using a polyclonal anti-H antibody to detect the H antigenic materials (lower panel).

since the actual model of morbillivirus-induced fusion activity suggests that, upon H/receptor binding, F dissociates from H to undergo refolding. Indeed, though F mutants L372A, L372W, and L372N mediated cell−cell fusion in Vero cells and were thus considered as hyperfusogenic compared to F^{wt}, fusion activity remained extremely limited throughout the whole cell monolayer (see Figure 2B). In fact, the results of the co-IP assays documented that F_0 precursors of all F L372 mutants associated with H to very similar extents as compared to F^{wt}.

Thus, even though F mutants exhibited substantial modifications compared to the parental F protein conformational state, the overall structural integrity of their metastable state appeared to be well conserved, since no drastic impairment in binding to the hemagglutinin protein was noticed.

F L372 Mutants Show a Lower Temperature Requirement for Fusion Activation. In order to determine whether F L372 mutations could modulate the energy required to activate the fusion process, plasma membrane fusion activity was assessed in function of increasing environmental temperatures. To indirectly measure F activation, dye transfer of labeled erythrocytes is usually performed (*11*, *13*, *24*, *40*). Since CDV-H does not hemagglutinate, at least not with canine erythrocytes (data not shown), we used Vero cells for measuring fusion efficiency. Furthermore, since these experiments were conducted in the presence of H^{wt}, Vero cells stably transfected with the CDV receptor SLAM were employed in order to enhance fusion efficiency and subsequent sensitivity of the assay. In addition, in order to track fusion events in a very short and sensitive manner, we developed a "two-color-based" fusion assay by first generating a stable cell line expressing both the receptor SLAM and the GFP protein (referred to as target Vero-SLAM-GFP cells). Second, we cotransfected BsrT7 cells with plasmids containing F and H as well as a red fluorescent protein (RFP) to label F/H-expressing cells (referred to as effector cells). It was expected that upon F/H/receptor-dependent pore formation, cytosolic contents of both cell lines would mix and consequently produce cells expressing both fluorescent proteins within several minutes. Thus, effector cells were cotransfected with RFP-, F^{wt}- (or F mutants), and H^{wt}-expressing plasmids. Following overnight incubation, effector cells were overlaid with target

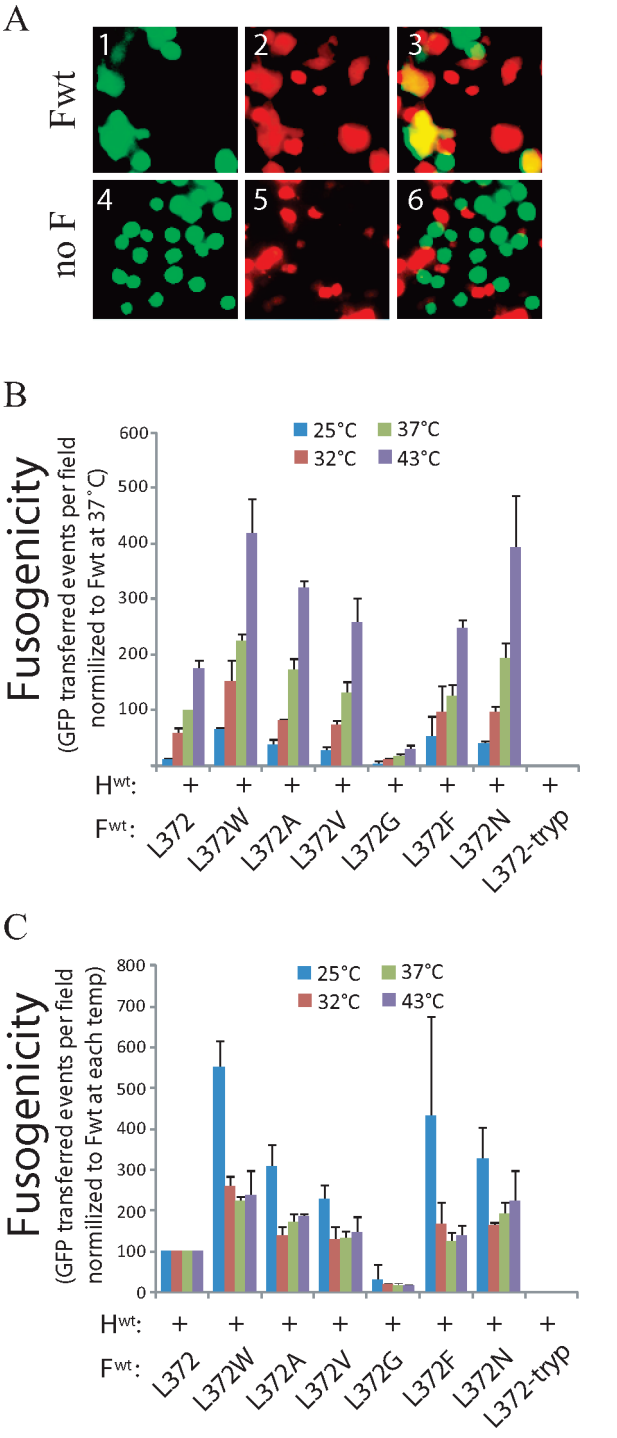

FIGURE 5: F mutants are more readily activated. (A) BsrT7 cells (effector cells) transfected with plasmid expressing F^{wt} or mutants in combination with H^{wt} and RFP were overlaid with Vero-SLAM-GFP (target cells) at 4 °C for 1 h, and both cell populations were then incubated for 15 min at 37 °C. Cell−cell fusion was monitored by merging images taken by confocal microscopy of green and red fluorescent light emission. Yellow images indicated pore formation and GFP transfer of Vero-SLAM-GFP cells into BsrT7-F-H-red cells. (B) Effector cells and target cells were incubated at 4 °C for 1 h, followed by 15 min at 25, 32, 37, and 43 °C. The four different temperatures are indicated in the inserted white box. GFP transfer events were counted in at least four different defined areas, and values were normalized to the number of total transfected cells in the same area. Means and standard deviations of three independent experiments in duplicate are shown. Data are normalized to values obtained for F^{wt} at 37 °C. (C) Identical to panel B, but data are normalized to values obtained for F^{wt} at 25, 32, 37, and 43 °C, respectively.

Vero-SLAM-GFP cells at 4 °C (a temperature which is restrictive for CDV-F-mediated fusion induction) during 1 h to synchronize fusion induction. This was followed by a transfer to higher temperatures to potentially initiate fusion activity. Figure 5A (panels 1−3) shows typical confocal microscopical images of cells expressing both GFP and RFP following fusion mediated by the F^{wt}/H^{wt}/SLAM tripartite complex at 37 °C. Importantly, no cell exhibiting both reporter fluorescent proteins was noticed in control experiments where H^{wt} was transfected alone (Figure 5A, panels 4−6), thereby validating our newly established fusion assay.

To determine the temperature required to activate the F^{wt} protein and derivative mutants, fusion activities were measured in function of incubation temperature increments. Figure 5B illustrates fusion efficiency of F^{wt} and F mutants at four different environmental temperatures (25, 32, 37, and 42 °C). Note that the values obtained for all F proteins were normalized to F^{wt}-mediated fusion activity at 37 °C. Interestingly, at all given temperatures, all F mutants (except L372G) exhibited increased fusogenicity as compared to F^{wt} at all tested temperatures. In particular, GFP/RFP transfer efficiency was higher with the three most hyperfusogenic F mutants (L372W, L372A, and L372N), as previously determined in the content mix assay and microscopical evaluation of syncytia formation. An F protein with the F_1/F_2 furin cleavage site mutated into a trypsin-dependent sequence (F^{wt}-tryp (*8*)) served as a control. In the absence of exogenous trypsin treatment no GFP/RFP transfer was observed at any given temperature in cells cotransfected with the latter F control mutant and H^{wt} (Figure 5B).

Importantly, when values from F mutants were normalized to the one of F^{wt} for each individual temperature, F mutants L372A, L372W, L372F, L372V, and L372N exhibited a significant increase in fusion activation only at the lowest temperature (25 °C, Figure 5C). Even the F L372G mutant exhibited a tendency for increased fusion activity at 25 °C as compared to higher temperatures (Figure 5C). The latter results support the notion that substituting the conserved leucine 372 residue in the wild-type CDV-F protein lowers the activation energy barrier required to induce plasma membrane fusion activity.

DISCUSSION

Virulent A75/17-CDV, which mediates a persistent demyelinating CNS infection in dogs, is characterized by a limited cell−cell fusion capacity. We previously reported a naturally occurring mutation in the wild-type fusion protein (F-A75/17) from leucine to tryptophan at position 372 causing markedly enhanced fusogenicity (*8*). This residue is located in a long intervening sequence between the HRA and HRB domains, which has been only poorly investigated so far.

In the present study we conducted a site-directed mutational analysis of the conserved leucine residue (L372) in CDV-F to investigate the molecular mechanisms by which this residue could control fusion activity. None but one (F L372G) of the six substitutions at position 372 caused any fundamental changes of F protein expression, processing, and cell surface targeting. Importantly, in the presence of the wild-type A75/17-H protein (which by itself limits cell−cell fusion in the absence of SLAM) F mutants L372W, L372A, and L372N exhibited hyperfusogenic phenotypes that could even achieve syncytium formation in Vero cells. When combined with the attachment protein of the closely related fusogenic Onderstepoort CDV strain, all mutants except F L372G elicited increased cell−cell fusion activity as compared to the parental F protein. Thus, our results clearly indicate that modifying hydrophobic or packing interactions of residue 372 in CDV-F resulted in a significant modulation of F functionality, underlining a crucial role of the specific properties of the conserved leucine 372 in controlling proper F activity.

Interestingly, F mutants were characterized by enhanced binding avidity to distinct conformation-dependent anti-CDV-F MAbs generated against a syncytium-inducing CDV strain (Convac (*31*)). It is conceivable that the activation kinetics of the highly fusogenic F mutants are different and that they may exhibit premature refolding toward the irreversible postfusion state. The epitopes recognized by the three different MAbs would subsequently be unmasked and accessible only in the activated F states (intermediates and/or postfusion). Interestingly, all three MAbs did neither exhibit any neutralizing activity against A75/17-CDV nor inhibit cell−cell fusion mediated by all F proteins in transient transfection assay (not shown), which may indicate that they did not recognize the prefusion F state. In addition, given the putative localization of residue 372 within the core structure of the globular head of CDV-F and the fact that all different mutations lead to an increase in MAb binding avidity, it is unlikely that L372 is directly involved in the three different epitopes recognized by the MAbs. Importantly, and in agreement with the hypothesis that F mutants may exhibit modified activation kinetics, we clearly demonstrated that all F L372 mutants substantially enhanced fusogenicity at low temperature. This result is consistent with the notion that the energy required to activate the fusion process is decreased for F proteins bearing a substitution at position 372. In turn, F mutants are more readily triggered by H at the cell surface. Taken together, we speculate that the highly conserved leucine 372 in the core structure of wild-type F is a key residue involved in controlling the stability of its metastable structure. Conversely, mutation of L372 can cause the premature conformational switch and expose conformational epitopes.

A direct correlation was observed between F mutants' capacities to induce cell−cell fusion and MAb binding efficiency. Unexpectedly, however, the least fusogenic mutant F L372G exhibited the greatest binding avidity for all three MAbs, which was even more pronounced in the absence of H coexpression. While MAb binding efficiency nicely reflected the degree of fusogenicity in five out of the six generated F mutants, we hypothesize that hyperreactivity of F mutant L372G with the MAbs would result from too much overall conformational change, which in turn would obviously affect functionality. On the other hand, even though conformational modifications were monitored for all F mutants, these differences had almost no impact on F/H interactions. Indeed, co-IP assays revealed that all F mutated proteins sustained efficient interactions with H, suggesting that at least the physical putative contacting domains with H of all metastable F proteins, prior to undergoing conformational changes, were not markedly modulated. This is also in agreement with our results showing that F mutated proteins (except F L372G) were properly expressed, processed, and cell surface targeted.

The conserved leucine in CDV-F is probably involved in a network of residues that are crucial for stabilizing the trimer prefusion state, thereby preventing premature F refolding. Consistent with this notion, the importance of trimer opening during the fusion process was documented in an engineered "trimer-locked" native influenza HA glycoprotein mutant (*41*), which

exhibited both structural rearrangements and membrane fusion deficiencies (*42*). Other residues in the ectodomain of paramyxovirus FGps have been shown to modulate the activation barrier by modulating the metastable F state (*12*, *22*, *24*, *40*, *43*). In addition, stabilizing and destabilizing residues are located all over the structure of influenza HA (*44*−*46*). The long cytoplasmic tails of paramyxovirus F and HIV Env/GP160 have also been demonstrated to stabilize the metastable structure by inside-out mechanisms (*24*, *47*). Taken together, it appears that stabilization of FGps' prefusion state by multiple subdomains is a general feature used by class I viral fusion proteins to control plasma membrane fusion activity.

How can L372 regulate the fusion process? On initiating the fusion process, the HRA domain of the fusion protein goes through a dramatic conformational change that involves refolding of 11 distinct segments. In the prefusion state, the HRA is held into monomeric subunits by stabilizing interactions with DIII core. For the transition to the postfusion conformation, the prefusion conformation of the trimer has to be destabilized. Early regulatory steps in this mechanism are thought to occur by melting of the HRB helices at the base of the head. In our newly generated CDV-F 3D model, residue L372 is located halfway between the head region in the last short helix of the helical bundle (HB) of the DIII core and may interact with neighboring C-terminal residues in helix H4 of an adjacent monomer (Figure 1C). Loss of these potential interactions may be involved in the subsequent destabilization of the trimer head. H4 is not dislocated over a large distance, does not change its secondary structure, but does change its tertiary structure by homotrimerization with the other H4 helices. It forms the initiation point for the coiled-coil formation and forms the base on top of which all the other 10 segments mount. The N-terminal end of H4 may function as a hinge because it is structurally fixed by the disulfide bridge between cysteine 180 and cysteine 307 that connects H4 to the DIII core (Figure 1C). In contrast, the C-terminal end of H4 is more free to move, and therefore, the putative lost contacts with L372 may unlock the head structure and allow the HRA to unroll.

In conclusion, we showed that a virulent and demyelinating morbillivirus evolved to maintain a hydrophobic leucine residue at position 372 in F. This position and probably other residues are involved in stabilizing the prefusion state of F. This stabilized F state interacts efficiently with H (at least prior to F_0 cleavage), is properly processed, and transported to the cell surface. The resulting elevated intrinsic F activation energy threshold limits cell−cell fusion induction by limiting the number of activated F trimers at the cell surface. As a result of the stabilized prefusion conformation of F^{wt}, syncytium formation is restricted in the absence of the SLAM receptor. Nevertheless, A75/17-CDV efficiently spreads in SLAM-negative brain cells with extremely limited free virus production (*4*). Consequently, CDV spread in the brain may depend on micropore induction and subsequent transfer of a nucleocapsid to neighboring cells, which ultimately may lead to a noncytolytic infection. Interestingly, noncytolytic infection has been suggested to impede proper immune detection *in vivo* and thus to sustain the establishment of morbillivirus-mediated persistence and chronic diseases (*4*).

ACKNOWLEDGMENT

We are grateful to Patrick Salmon, Laurent Roux, D. Garcin, and V. von Messling for having provided the pRRL lenti plasmid system, the pTM-Luc plasmid, the RFP gene, and the Vero-SLAM cells, respectively.

REFERENCES

1. Lamb, R. A., and Kolakofsky, D. (2001) Paramyxoviridae: the viruses and their replication, in Fields virology (Fileds, B. N., Knipe, D. M., Howley, P. M., and Griffin, D. E., Eds.) 4th ed., pp 1305−1340, Lippincott-Raven, Philadelphia, PA.
2. Lamb, R. A. (1993) Paramyxovirus fusion: a hypothesis for changes. *Virology 197*, 1–11.
3. Vandevelde, M., Zurbriggen, A., Higgins, R. J., and Palmer, D. (1985) Spread and distribution of viral antigen in nervous canine distemper. *Acta Neuropathol.* (*Berlin*) *67*, 211–218.
4. Zurbriggen, A., Graber, H. U., Wagner, A., and Vandevelde, M. (1995) Canine distemper virus persistence in the nervous system is associated with noncytolytic selective virus spread. *J. Virol. 69*, 1678–1686.
5. Zurbriggen, A., Graber, H. U., and Vandevelde, M. (1995) Selective spread and reduced virus release leads to canine distemper virus persistence in the nervous system. *Vet. Microbiol. 44*, 281–288.
6. Wiener, D., Plattet, P., Cherpillod, P., Zipperle, L., Doherr, M. G., Vandevelde, M., and Zurbriggen, A. (2007) Synergistic inhibition in cell-cell fusion mediated by the matrix and nucleocapsid protein of canine distemper virus. *Virus Res. 129*, 145–154.
7. Plattet, P., Rivals, J. P., Zuber, B., Brunner, J. M., Zurbriggen, A., and Wittek, R. (2005) The fusion protein of wild-type canine distemper virus is a major determinant of persistent infection. *Virology 337*, 312–326.
8. Plattet, P., Cherpillod, P., Wiener, D., Zipperle, L., Vandevelde, M., Wittek, R., and Zurbriggen, A. (2007) Signal peptide and helical bundle domains of virulent canine distemper virus fusion protein restrict fusogenicity. *J. Virol. 81*, 11413–11425.
9. Bolt, G., and Pedersen, I. R. (1998) The role of subtilisin-like proprotein convertases for cleavage of the measles virus fusion glycoprotein in different cell types. *Virology 252*, 387–398.
10. Yin, H. S., Wen, X., Paterson, R. G., Lamb, R. A., and Jardetzky, T. S. (2006) Structure of the parainfluenza virus 5 F protein in its metastable, prefusion conformation. *Nature 439*, 38–44.
11. Russell, C. J., Jardetzky, T. S., and Lamb, R. A. (2001) Membrane fusion machines of paramyxoviruses: capture of intermediates of fusion. *EMBO J. 20*, 4024–4034.
12. Russell, C. J., Kantor, K. L., Jardetzky, T. S., and Lamb, R. A. (2003) A dual-functional paramyxovirus F protein regulatory switch segment: activation and membrane fusion. *J. Cell Biol. 163*, 363–374.
13. Luque, L. E., and Russell, C. J. (2007) Spring-loaded heptad repeat residues regulate the expression and activation of paramyxovirus fusion protein. *J. Virol. 81*, 3130–3141.
14. Joshi, S. B., Dutch, R. E., and Lamb, R. A. (1998) A core trimer of the paramyxovirus fusion protein: parallels to influenza virus hemagglutinin and HIV-1 gp41. *Virology 248*, 20–34.
15. Lambert, D. M., Barney, S., Lambert, A. L., Guthrie, K., Medinas, R., Davis, D. E., Bucy, T., Erickson, J., Merutka, G., and Petteway, S. R.Jr. (1996) Peptides from conserved regions of paramyxovirus fusion (F) proteins are potent inhibitors of viral fusion. *Proc. Natl. Acad. Sci. U.S.A. 93*, 2186–2191.
16. Rapaport, D., Ovadia, M., and Shai, Y. (1995) A synthetic peptide corresponding to a conserved heptad repeat domain is a potent inhibitor of Sendai virus-cell fusion: an emerging similarity with functional domains of other viruses. *EMBO J. 14*, 5524–5531.
17. Wild, T. F., and Buckland, R. (1997) Inhibition of measles virus infection and fusion with peptides corresponding to the leucine zipper region of the fusion protein. *J. Gen. Virol. 78* (Part 1), 107–111.
18. Yao, Q., and Compans, R. W. (1996) Peptides corresponding to the heptad repeat sequence of human parainfluenza virus fusion protein are potent inhibitors of virus infection. *Virology 223*, 103–112.
19. Young, J. K., Hicks, R. P., Wright, G. E., and Morrison, T. G. (1997) Analysis of a peptide inhibitor of paramyxovirus (NDV) fusion using biological assays, NMR, and molecular modeling. *Virology 238*, 291–304.
20. Young, J. K., Li, D., Abramowitz, M. C., and Morrison, T. G. (1999) Interaction of peptides with sequences from the Newcastle disease virus fusion protein heptad repeat regions. *J. Virol. 73*, 5945–5956.
21. Dutch, R. E., and Lamb, R. A. (2001) Deletion of the cytoplasmic tail of the fusion protein of the paramyxovirus simian virus 5 affects fusion pore enlargement. *J. Virol. 75*, 5363–5369.
22. Seth, S., Goodman, A. L., and Compans, R. W. (2004) Mutations in multiple domains activate paramyxovirus F protein-induced fusion. *J. Virol. 78*, 8513–8523.

23. Seth, S., Vincent, A., and Compans, R. W. (2003) Mutations in the cytoplasmic domain of a paramyxovirus fusion glycoprotein rescue syncytium formation and eliminate the hemagglutinin-neuraminidase protein requirement for membrane fusion. *J. Virol. 77*, 167–178.
24. Waning, D. L., Russell, C. J., Jardetzky, T. S., and Lamb, R. A. (2004) Activation of a paramyxovirus fusion protein is modulated by inside-out signaling from the cytoplasmic tail. *Proc. Natl. Acad. Sci. U.S.A. 101*, 9217–9222.
25. Muhlebach, M. D., Leonard, V. H., and Cattaneo, R. (2008) The measles virus fusion protein transmembrane region modulates availability of an active glycoprotein complex and fusion efficiency. *J. Virol. 82*, 11437–11445.
26. Gardner, A. E., Martin, K. L., and Dutch, R. E. (2007) A conserved region between the heptad repeats of paramyxovirus fusion proteins is critical for proper F protein folding. *Biochemistry 46*, 5094–5105.
27. Cherpillod, P., Beck, K., Zurbriggen, A., and Wittek, R. (1999) Sequence analysis and expression of the attachment and fusion proteins of canine distemper virus wild-type strain A75/17. *J. Virol. 73*, 2263–2269.
28. Dayer, A. G., Jenny, B., Sauvain, M. O., Potter, G., Salmon, P., Zgraggen, E., Kanemitsu, M., Gascon, E., Sizonenko, S., Trono, D., and Kiss, J. Z. (2007) Expression of FGF-2 in neural progenitor cells enhances their potential for cellular brain repair in the rodent cortex. *Brain 130*, 2962–2976.
29. Nussbaum, O., Broder, C. C., and Berger, E. A. (1994) Fusogenic mechanisms of enveloped-virus glycoproteins analyzed by a novel recombinant vaccinia virus-based assay quantitating cell fusion-dependent reporter gene activation. *J. Virol. 68*, 5411–5422.
30. Sutter, G., Ohlmann, M., and Erfle, V. (1995) Non-replicating vaccinia vector efficiently expresses bacteriophage T7 RNA polymerase. *FEBS Lett. 371*, 9–12.
31. Orvell, C., Sheshberadaran, H., and Norrby, E. (1985) Preparation and characterization of monoclonal antibodies directed against four structural components of canine distemper virus. *J. Gen. Virol. 66* (Part 3), 443–456.
32. Guex, N., and Peitsch, M. C. (1997) SWISS-MODEL and the Swiss-PdbViewer: an environment for comparative protein modeling. *Electrophoresis 18*, 2714–2723.
33. Peitsch, M. C. (1996) ProMod and Swiss-Model: Internet-based tools for automated comparative protein modelling. *Biochem. Soc. Trans. 24*, 274–279.
34. Hooft, R. W., Vriend, G., Sander, C., and Abola, E. E. (1996) Errors in protein structures. *Nature 381*, 272.
35. Seki, F., Ono, N., Yamaguchi, R., and Yanagi, Y. (2003) Efficient isolation of wild strains of canine distemper virus in Vero cells expressing canine SLAM (CD150) and their adaptability to marmoset B95a cells. *J. Virol. 77*, 9943–9950.
36. von Messling, V., Zimmer, G., Herrler, G., Haas, L., and Cattaneo, R. (2001) The hemagglutinin of canine distemper virus determines tropism and cytopathogenicity. *J. Virol. 75*, 6418–6427.
37. Plemper, R. K., Hammond, A. L., Gerlier, D., Fielding, A. K., and Cattaneo, R. (2002) Strength of envelope protein interaction modulates cytopathicity of measles virus. *J. Virol. 76*, 5051–5061.
38. Lee, J. K., Prussia, A., Paal, T., White, L. K., Snyder, J. P., and Plemper, R. K. (2008) Functional interaction between paramyxovirus fusion and attachment proteins. *J. Biol. Chem. 283*, 16561–16572.
39. Corey, E. A., and Iorio, R. M. (2009) Measles virus attachment proteins with impaired ability to bind CD46 interact more efficiently with the homologous fusion protein. *Virology 383*, 1–5.
40. Russell, C. J., Jardetzky, T. S., and Lamb, R. A. (2004) Conserved glycine residues in the fusion peptide of the paramyxovirus fusion protein regulate activation of the native state. *J. Virol. 78*, 13727–13742.
41. Godley, L., Pfeifer, J., Steinhauer, D., Ely, B., Shaw, G., Kaufmann, R., Suchanek, E., Pabo, C., Skehel, J. J., and Wiley, D. C. (1992) Introduction of intersubunit disulfide bonds in the membrane-distal region of the influenza hemagglutinin abolishes membrane fusion activity. *Cell 68*, 635–645.
42. Kemble, G. W., Bodian, D. L., Rose, J., Wilson, I. A., and White, J. M. (1992) Intermonomer disulfide bonds impair the fusion activity of influenza virus hemagglutinin. *J. Virol. 66*, 4940–4950.
43. Paterson, R. G., Russell, C. J., and Lamb, R. A. (2000) Fusion protein of the paramyxovirus SV5: destabilizing and stabilizing mutants of fusion activation. *Virology 270*, 17–30.
44. Thoennes, S., Li, Z. N., Lee, B. J., Langley, W. A., Skehel, J. J., Russell, R. J., and Steinhauer, D. A. (2008) Analysis of residues near the fusion peptide in the influenza hemagglutinin structure for roles in triggering membrane fusion. *Virology 370*, 403–414.
45. Daniels, R. S., Downie, J. C., Hay, A. J., Knossow, M., Skehel, J. J., Wang, M. L., and Wiley, D. C. (1985) Fusion mutants of the influenza virus hemagglutinin glycoprotein. *Cell 40*, 431–439.
46. Doms, R. W., Gething, M. J., Henneberry, J., White, J., and Helenius, A. (1986) Variant influenza virus hemagglutinin that induces fusion at elevated pH. *J. Virol. 57*, 603–613.
47. Edwards, T. G., Wyss, S., Reeves, J. D., Zolla-Pazner, S., Hoxie, J. A., Doms, R. W., and Baribaud, F. (2002) Truncation of the cytoplasmic domain induces exposure of conserved regions in the ectodomain of human immunodeficiency virus type 1 envelope protein. *J. Virol. 76*, 2683–2691.